

9

FEM FOR 3D SOLIDS

9.1 INTRODUCTION

A three-dimensional (3D) solid element can be considered to be the most general of all solid finite elements because all the field variables are dependent of x , y and z . An example of a 3D solid structure under loading is shown in Figure 9.1. As can be seen, the force vectors here can be in any arbitrary direction in space. A 3D solid can also have any arbitrary shape, material properties and boundary conditions in space. As such, there are altogether six possible stress components, three normal and three shear, that need to be taken into consideration. Typically, a 3D solid element can be a tetrahedron or hexahedron in shape with either flat or curved surfaces. Each node of the element will have three translational degrees of freedom. The element can thus deform in all three directions in space.

Since the 3D element is said to be the most general solid element, the truss, beam, plate, 2D solid and shell elements can all be considered to be special cases of the 3D element. So, why is there a need to develop all the other elements? Why not just use the 3D element to model everything? Theoretically, yes, the 3D element can actually be used to model all kinds of structural components, including trusses, beams, plates, shells and so on. However, it can be very tedious in geometry creation and meshing. Furthermore, it is also most demanding on computer resources. Hence, the general rule of thumb is, that when a

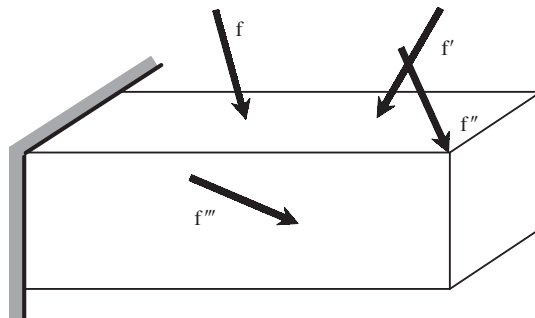


Figure 9.1. Example of a 3D solid under loadings.

structure can be assumed within acceptable tolerances to be simplified into a 1D (trusses, beams and frames) or 2D (2D solids and plates) structure, always do so. The creation of a 1D or 2D FEM model is much easier and efficient. Use 3D solid elements only when we have no other choices. The formulation of 3D solids elements is straightforward, because it is basically an extension of 2D solids elements. All the techniques used in 2D solids can be utilized, except that all the variables are now functions of x , y and z . The basic concepts, procedures and formulations for 3D solid elements can also be found in many existing books (see, e.g., Washizu, 1981; Rao, 1999; Zienkiewicz and Taylor, 2000; etc.).

9.2 TETRAHEDRON ELEMENT

9.2.1 Strain Matrix

Consider the same 3D solid structure as Figure 9.1, whose domain is divided in a proper manner into a number of *tetrahedron* elements (Figure 9.2) with four nodes and four surfaces, as shown in Figure 9.3. A tetrahedron element has four nodes, each having three DOFs

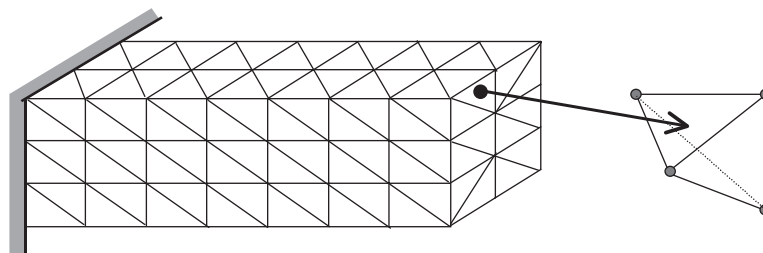


Figure 9.2. Solid block divided into four-node tetrahedron elements.

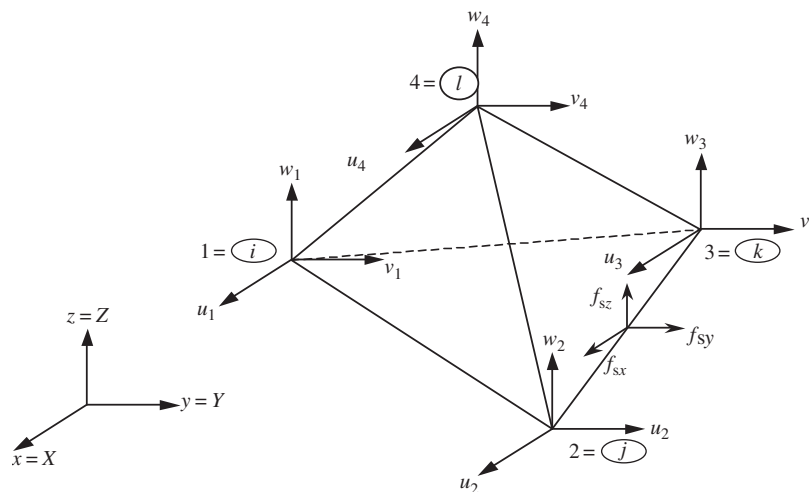


Figure 9.3. A tetrahedron element.

(u , v and w), making the total DOFs in a tetrahedron element twelve, as shown in Figure 9.3. The nodes are numbered 1, 2, 3 and 4 by the right-hand rule. The local Cartesian coordinate system for a tetrahedron element can usually be the same as the global coordinate system, as there are no advantages in having a separate local Cartesian coordinate system. In an element, the displacement vector \mathbf{U} is a function of the coordinate x , y and z , and is interpolated by shape functions in the following form, which should by now be shown to be part and parcel of the finite element method:

$$\mathbf{U}^h(x, y, z) = \mathbf{N}(x, y, z)\mathbf{d}_e \quad (9.1)$$

where the nodal displacement vector, \mathbf{d}_e , is given as

$$\mathbf{d}_e = \left\{ \begin{array}{l} u_1 \\ v_1 \\ w_1 \\ u_2 \\ v_2 \\ w_2 \\ u_3 \\ v_3 \\ w_3 \\ u_4 \\ v_4 \\ w_4 \end{array} \right\} \begin{array}{l} \left. \vphantom{\begin{array}{l} u_1 \\ v_1 \\ w_1 \end{array}} \right\} \text{displacements at node 1} \\ \left. \vphantom{\begin{array}{l} u_2 \\ v_2 \\ w_2 \end{array}} \right\} \text{displacements at node 2} \\ \left. \vphantom{\begin{array}{l} u_3 \\ v_3 \\ w_3 \end{array}} \right\} \text{displacements at node 3} \\ \left. \vphantom{\begin{array}{l} u_4 \\ v_4 \\ w_4 \end{array}} \right\} \text{displacements at node 4} \end{array} \quad (9.2)$$

and the matrix of shape functions has the form

$$\mathbf{N} = \begin{bmatrix} \overbrace{N_1 \ 0 \ 0}^{\text{node 1}} & \overbrace{N_2 \ 0 \ 0}^{\text{node 2}} & \overbrace{N_3 \ 0 \ 0}^{\text{node 3}} & \overbrace{N_4 \ 0 \ 0}^{\text{node 4}} \\ 0 \ N_1 \ 0 & 0 \ N_2 \ 0 & 0 \ N_3 \ 0 & 0 \ N_4 \ 0 \\ 0 \ 0 \ N_1 & 0 \ 0 \ N_2 & 0 \ 0 \ N_3 & 0 \ 0 \ N_4 \end{bmatrix} \quad (9.3)$$

To develop the shape functions, we make use of what is known as the *volume coordinates*, which is a natural extension from the area coordinates for 2D solids. The use of the volume coordinates makes it more convenient for shape function construction and element matrix integration. The volume coordinate for node 1 is defined as

$$L_1 = \frac{V_{P234}}{V_{1234}} \quad (9.4)$$

where V_{P234} and V_{1234} denote, respectively, the volumes of the tetrahedrons P234 and 1234, as shown in Figure 9.4. The volume coordinate for node 2-4 can also be defined in the same

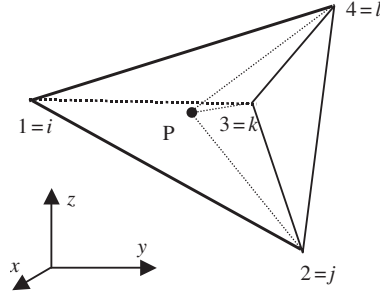


Figure 9.4. Volume coordinates for tetrahedron elements.

manner:

$$L_2 = \frac{V_{P134}}{V_{1234}}, \quad L_3 = \frac{V_{P124}}{V_{1234}}, \quad L_4 = \frac{V_{P123}}{V_{1234}} \quad (9.5)$$

The volume coordinate can also be viewed as the ratio between the distance of the point P and point 1 to the plane 234:

$$L_1 = \frac{d_{P-234}}{d_{1-234}}, \quad L_2 = \frac{d_{P-134}}{d_{1-234}}, \quad L_3 = \frac{d_{P-124}}{d_{1-234}}, \quad L_4 = \frac{d_{P-123}}{d_{1-234}} \quad (9.6)$$

It can easily be confirmed that

$$L_1 + L_2 + L_3 + L_4 = 1 \quad (9.7)$$

since

$$V_{P234} + V_{P134} + V_{P124} + V_{P123} = V_{1234} \quad (9.8)$$

It can also easily be confirmed that

$$L_i = \begin{cases} 1 & \text{at the home node } i \\ 0 & \text{at the remote nodes } jkl \end{cases} \quad (9.9)$$

Using Eq. (9.9), the relationship between the volume coordinates and Cartesian coordinates can be easily derived:

$$\begin{aligned} x &= L_1x_1 + L_2x_2 + L_3x_3 + L_4x_4 \\ y &= L_1y_1 + L_2y_2 + L_3y_3 + L_4y_4 \\ z &= L_1z_1 + L_2z_2 + L_3z_3 + L_4z_4 \end{aligned} \quad (9.10)$$

Equations (9.7) and (9.10) can then be expressed as a single matrix equation as follows:

$$\begin{Bmatrix} 1 \\ x \\ y \\ z \end{Bmatrix} = \begin{bmatrix} 1 & 1 & 1 & 1 \\ x_1 & x_2 & x_3 & x_4 \\ y_1 & y_2 & y_3 & y_4 \\ z_1 & z_2 & z_3 & z_4 \end{bmatrix} \begin{Bmatrix} L_1 \\ L_2 \\ L_3 \\ L_4 \end{Bmatrix} \quad (9.11)$$

The inversion of Eq. (9.11) will give

$$\begin{Bmatrix} L_1 \\ L_2 \\ L_3 \\ L_4 \end{Bmatrix} = \frac{1}{6V} \begin{bmatrix} a_1 & b_1 & c_1 & d_1 \\ a_2 & b_2 & c_2 & d_2 \\ a_3 & b_3 & c_3 & d_3 \\ a_4 & b_4 & c_4 & d_4 \end{bmatrix} \begin{Bmatrix} 1 \\ x \\ y \\ z \end{Bmatrix} \quad (9.12)$$

where

$$\begin{aligned} a_i &= \det \begin{bmatrix} x_j & y_j & z_j \\ x_k & y_k & z_k \\ x_l & y_l & z_l \end{bmatrix}, & b_i &= -\det \begin{bmatrix} 1 & y_j & z_j \\ 1 & y_k & z_k \\ 1 & y_l & z_l \end{bmatrix} \\ c_i &= -\det \begin{bmatrix} y_j & 1 & z_j \\ y_k & 1 & z_k \\ y_l & 1 & z_l \end{bmatrix}, & d_i &= -\det \begin{bmatrix} y_j & z_j & 1 \\ y_k & z_k & 1 \\ y_l & z_l & 1 \end{bmatrix} \end{aligned} \quad (9.13)$$

in which the subscript i varies from 1 to 4, and j, k and l are determined by a cyclic permutation in the order of i, j, k, l . For example, if $i = 1$, then $j = 2, k = 3, l = 4$. When $i = 2$, then $j = 3, k = 4, l = 1$. The volume of the tetrahedron element V can be obtained by

$$V = \frac{1}{6} \times \det \begin{bmatrix} 1 & x_i & y_i & z_i \\ 1 & x_j & y_j & z_j \\ 1 & x_k & y_k & z_k \\ 1 & x_l & y_l & z_l \end{bmatrix} \quad (9.14)$$

The properties of L_i , as depicted in Eqs. (9.6) to (9.9), show that L_i can be used as the shape function of a four-nodal tetrahedron element:

$$N_i = L_i = \frac{1}{6V}(a_i + b_i x + c_i y + d_i z) \quad (9.15)$$

It can be seen from above that the shape function is a linear function of x, y and z , hence, the four-nodal tetrahedron element is a linear element. Note that from Eq. (9.14), the moment matrix of the linear basis functions will never be singular, unless the volume of the element is zero (or the four nodes of the element are in a plane). Based on Lemmas 2 and 3, we can be sure that the shape functions given by Eq. (9.15) satisfy the sufficient requirement of FEM shape functions.

It was mentioned that there are six stresses in a 3D element in total. The stress components are $\{\sigma_{xx} \ \sigma_{yy} \ \sigma_{zz} \ \sigma_{yz} \ \sigma_{xz} \ \sigma_{xy}\}$. To get the corresponding strains, $\{\varepsilon_{xx} \ \varepsilon_{yy} \ \varepsilon_{zz} \ \varepsilon_{yz} \ \varepsilon_{xz} \ \varepsilon_{xy}\}$, we can substitute Eq. (9.1) into Eq. (2.5):

$$\varepsilon = \mathbf{LU} = \mathbf{LNd}_e = \mathbf{Bd}_e \quad (9.16)$$

where the strain matrix \mathbf{B} is given by

$$\mathbf{B} = \mathbf{LN} = \begin{bmatrix} \partial/\partial x & 0 & 0 \\ 0 & \partial/\partial y & 0 \\ 0 & 0 & \partial/\partial z \\ 0 & \partial/\partial z & \partial/\partial y \\ \partial/\partial z & 0 & \partial/\partial x \\ \partial/\partial y & \partial/\partial x & 0 \end{bmatrix} \mathbf{N} \quad (9.17)$$

Using Eq. (9.3), the strain matrix, \mathbf{B} , can be obtained as

$$\mathbf{B} = \frac{1}{2V} \begin{bmatrix} b_1 & 0 & 0 & b_2 & 0 & 0 & b_3 & 0 & 0 & b_4 & 0 & 0 \\ 0 & c_1 & 0 & 0 & c_2 & 0 & 0 & c_3 & 0 & 0 & c_4 & 0 \\ 0 & 0 & d_1 & 0 & 0 & d_2 & 0 & 0 & d_3 & 0 & 0 & d_4 \\ c_1 & b_1 & 0 & c_2 & b_2 & 0 & c_3 & b_3 & 0 & c_4 & b_4 & 0 \\ 0 & d_1 & c_1 & 0 & d_2 & c_2 & 0 & d_3 & c_3 & 0 & d_4 & c_4 \\ d_1 & 0 & b_1 & d_2 & 0 & b_2 & d_3 & 0 & b_3 & d_4 & 0 & b_4 \end{bmatrix} \quad (9.18)$$

It can be seen that the strain matrix for a linear tetrahedron element is a constant matrix. This implies that the strain within a linear tetrahedron element is constant, and thus so is the stress. Therefore, the linear tetrahedron elements are also often referred to as a *constant strain element* or *constant stress element*, similar to the case of 2D linear triangular elements.

9.2.2 Element Matrices

Once the strain matrix has been obtained, the stiffness matrix \mathbf{k}_e for 3D solid elements can be obtained by substituting Eq. (9.18) into Eq. (3.71). Since the strain is constant, the element strain matrix is obtained as

$$\mathbf{k}_e = \int_{V_e} \mathbf{B}^T \mathbf{cB} \, dV = V_e \mathbf{B}^T \mathbf{cB} \quad (9.19)$$

Note that the material constant matrix \mathbf{c} is given generally by Eq. (2.9).

The mass matrix can similarly be obtained using Eq. (3.75):

$$\mathbf{m}_e = \int_{V_e} \rho \mathbf{N}^T \mathbf{N} \, dV = \int_{V_e} \rho \begin{bmatrix} \mathbf{N}_{11} & \mathbf{N}_{12} & \mathbf{N}_{13} & \mathbf{N}_{14} \\ \mathbf{N}_{21} & \mathbf{N}_{22} & \mathbf{N}_{23} & \mathbf{N}_{24} \\ \mathbf{N}_{31} & \mathbf{N}_{32} & \mathbf{N}_{33} & \mathbf{N}_{34} \\ \mathbf{N}_{41} & \mathbf{N}_{42} & \mathbf{N}_{43} & \mathbf{N}_{44} \end{bmatrix} dV \quad (9.20)$$

where

$$\mathbf{N}_{ij} = \begin{bmatrix} N_i N_j & 0 & 0 \\ 0 & N_i N_j & 0 \\ 0 & 0 & N_i N_j \end{bmatrix} \quad (9.21)$$

Using the following formula [Eisenberg and Malvern, 1973],

$$\int_{V_e} L_1^m L_2^n L_3^p L_4^q \, dV = \frac{m!n!p!q!}{(m+n+p+q+3)!} 6V_e \quad (9.22)$$

we can conveniently evaluate the integral in Eq. (9.20) to give

$$\mathbf{m}_e = \frac{\rho V_e}{20} \begin{bmatrix} 2 & 0 & 0 & 1 & 0 & 0 & 1 & 0 & 0 & 1 & 0 & 0 \\ & 2 & 0 & 0 & 1 & 0 & 0 & 1 & 0 & 0 & 1 & 0 \\ & & 2 & 0 & 0 & 1 & 0 & 0 & 1 & 0 & 0 & 1 \\ & & & 2 & 0 & 0 & 1 & 0 & 0 & 1 & 0 & 0 \\ & & & & 2 & 0 & 0 & 1 & 0 & 0 & 1 & 0 \\ & & & & & 2 & 0 & 0 & 1 & 0 & 0 & 1 \\ & & & & & & 2 & 0 & 0 & 1 & 0 & 0 \\ & & & & & & & 2 & 0 & 0 & 1 & 0 \\ & & & & & & & & 2 & 0 & 0 & 1 \\ & & & & & & & & & 2 & 0 & 0 \\ & & & & & & & & & & 2 & 0 \\ & & & & & & & & & & & 2 \\ & & & & & & & & & & & & 2 \end{bmatrix} \quad (9.23)$$

An alternative way to calculate the mass matrix for 3D solid elements is to use a special natural coordinate system, which is defined as shown in Figures 9.5–9.7. In Figure 9.5, the plane of $\xi = \text{constant}$ is defined in such a way that the edge P–Q stays parallel to the edge 2–3 of the element, and point 4 coincides with point 4 of the element. When P moves to point 1, $\xi = 0$, and when P moves to point 2, $\xi = 1$. In Figure 9.6, the plane of $\eta = \text{constant}$ is defined in such a way that the edge 1–4 on the triangle coincides with the edge 1–4 of the element, and point P stays on the edge 2–3 of the element. When P moves to point 2, $\eta = 0$, and when P moves to point 3, $\eta = 1$. The plane of $\zeta = \text{constant}$ is defined in Figure 9.7, in such a way that the plane P–Q–R stays parallel to the plane 1–2–3 of the element, and when P moves to point 4, $\zeta = 0$, and when P moves to point 2, $\zeta = 1$. In addition, the

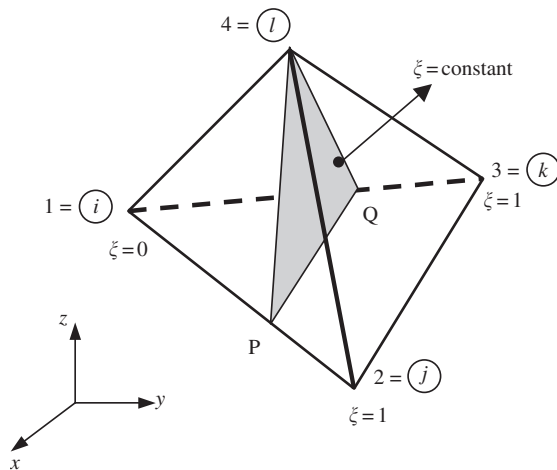


Figure 9.5. Natural coordinate, where $\xi = \text{constant}$.

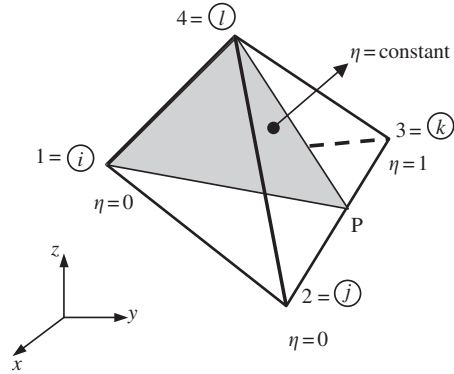


Figure 9.6. Natural coordinate, where $\eta = \text{constant}$.

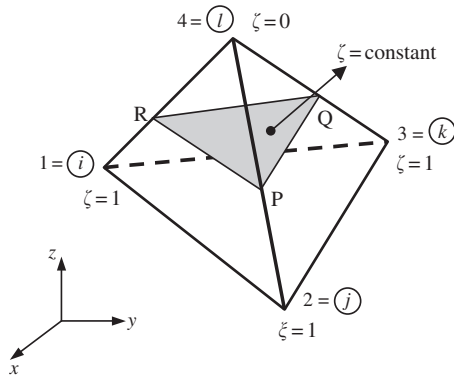


Figure 9.7. Natural coordinate, where $\zeta = \text{constant}$.

plane 1–2–3 on the element sits on the x – y plane. Therefore, the relationship between xyz and $\xi\eta\zeta$ can be obtained in the following steps:

In Figure 9.8, the coordinates at point P are first interpolated using the x , y and z coordinates at points 2 and 3:

$$\begin{aligned} x_P &= \eta(x_3 - x_2) + x_2 \\ y_P &= \eta(y_3 - y_2) + y_2 \\ z_P &= 0 \end{aligned} \tag{9.24}$$

The coordinates at point B are then interpolated using the x , y and z coordinates at points 1 and P:

$$\begin{aligned} x_B &= \xi(x_P - x_1) + x_1 = \xi\eta(x_3 - x_2) + \xi(x_2 - x_1) + x_1 \\ y_B &= \xi(y_P - y_1) + y_1 = \xi\eta(y_3 - y_2) + \xi(y_2 - y_1) + y_1 \\ z_B &= 0 \end{aligned} \tag{9.25}$$

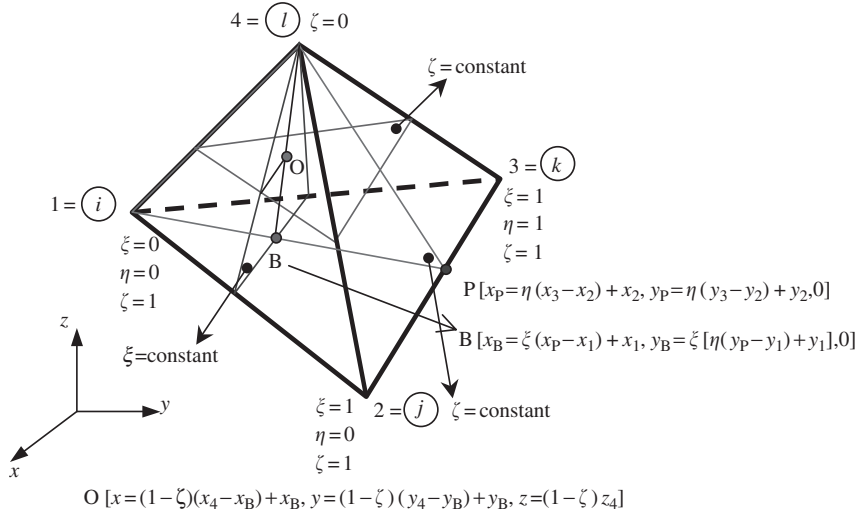


Figure 9.8. Cartesian coordinates xyz of point O in term of $\xi\eta\zeta$.

The coordinates at point O are finally interpolated using the x , y and z coordinates at points 4 and B :

$$\begin{aligned}
 x &= x_4 - \zeta(x_4 - x_B) = x_4 - \zeta(x_4 - x_1) + \xi\zeta(x_2 - x_1) - \xi\zeta(x_2 - x_3) \\
 y &= y_4 - \zeta(y_4 - y_B) = y_4 - \zeta(y_4 - y_1) + \xi\zeta(y_2 - y_1) - \xi\zeta(y_2 - y_3) \\
 z &= (1 - \zeta)z_4
 \end{aligned} \tag{9.26}$$

With this special natural coordinate system, the shape functions in the matrix of Eq. (9.3) can be written by inspection as

$$\begin{aligned}
 N_1 &= (1 - \xi)\zeta \\
 N_2 &= \xi\eta\zeta \\
 N_3 &= \xi\zeta(1 - \eta) \\
 N_4 &= (1 - \zeta)
 \end{aligned} \tag{9.27}$$

The Jacobian matrix between xyz and $\xi\eta\zeta$ is required, and is given as

$$\mathbf{J} = \begin{bmatrix} \partial x / \partial \xi & \partial x / \partial \eta & \partial x / \partial \zeta \\ \partial y / \partial \xi & \partial y / \partial \eta & \partial y / \partial \zeta \\ \partial z / \partial \xi & \partial z / \partial \eta & \partial z / \partial \zeta \end{bmatrix} \tag{9.28}$$

Using Eqs. (9.26) and (9.27), the determinate of the Jacobian can be found to be

$$\det[\mathbf{J}] = \begin{vmatrix} \zeta x_{21} + \eta\zeta x_{31} & \xi\zeta x_{31} & -x_{41} + \xi x_{21} + \xi\eta x_{31} \\ \zeta y_{21} + \eta\zeta y_{31} & \xi\zeta y_{31} & -y_{41} + \xi y_{21} + \xi\eta y_{31} \\ 0 & z_4 & 0 \end{vmatrix} = -6V\xi\zeta^2 \tag{9.29}$$

The mass matrix can now be obtained as

$$\mathbf{m}_e = \int_{V_e} \rho \mathbf{N}^T \mathbf{N} dV = \int_0^1 \int_0^1 \int_0^1 \rho \mathbf{N}^T \mathbf{N} \det[\mathbf{J}] d\xi d\eta d\zeta \quad (9.30)$$

which gives

$$\mathbf{m}_e = -6V_e \rho \int_0^1 \int_0^1 \int_0^1 \xi \zeta^2 \begin{bmatrix} \mathbf{N}_{11} & \mathbf{N}_{12} & \mathbf{N}_{13} & \mathbf{N}_{14} \\ \mathbf{N}_{21} & \mathbf{N}_{22} & \mathbf{N}_{23} & \mathbf{N}_{24} \\ \mathbf{N}_{31} & \mathbf{N}_{32} & \mathbf{N}_{33} & \mathbf{N}_{34} \\ \mathbf{N}_{41} & \mathbf{N}_{42} & \mathbf{N}_{43} & \mathbf{N}_{44} \end{bmatrix} d\xi d\eta d\zeta \quad (9.31)$$

where \mathbf{N}_{ij} is given by Eq. (9.21), but in which the shape functions should be defined by Eq. (9.27). Evaluating the integrals in Eq. (9.31) would give the same mass matrix as in Eq. (9.23).

The nodal force vector for 3D solid elements can be obtained using Eqs. (3.78), (3.79) and (3.81). Suppose the element is loaded by a distributed force \mathbf{f}_s on the edge 2–3 of the element as shown in Figure 9.3; the nodal force vector becomes

$$\mathbf{f}_e = \int_l [\mathbf{N}]^T \Big|_{3-4} \begin{Bmatrix} f_{sx} \\ f_{sy} \\ f_{sz} \end{Bmatrix} dl \quad (9.32)$$

If the load is uniformly distributed, f_{sx} , f_{sy} and f_{sz} are constants, and the above equation becomes

$$\mathbf{f}_e = \frac{1}{2} l_{3-4} \begin{Bmatrix} \{\mathbf{0}\}_{3 \times 1} \\ \{\mathbf{0}\}_{3 \times 1} \\ \begin{Bmatrix} f_{sx} \\ f_{sy} \\ f_{sz} \end{Bmatrix} \\ \begin{Bmatrix} f_{sx} \\ f_{sy} \\ f_{sz} \end{Bmatrix} \\ \{\mathbf{0}\}_{3 \times 1} \\ \{\mathbf{0}\}_{3 \times 1} \\ \{\mathbf{0}\}_{3 \times 1} \\ \{\mathbf{0}\}_{3 \times 1} \end{Bmatrix} \quad (9.33)$$

where l_{3-4} is the length of the edge 3–4. Equation (9.33) implies that the distributed forces are equally divided and applied at the two nodes. This conclusion also applies to evenly distributed surface forces applied on any face of the element, and to evenly distributed body force applied on the entire body of the element. Finally, the stiffness matrix, \mathbf{k}_e , the mass matrix, \mathbf{m}_e , and the nodal force vector, \mathbf{f}_e , can be used directly to assemble the global FE equation, Eq. (3.96), without going through a coordinate transformation.

9.3 HEXAHEDRON ELEMENT

9.3.1 Strain Matrix

Consider now a 3D domain, which is divided in a proper manner into a number of *hexahedron elements* with eight nodes and six surfaces, as shown in Figure 9.9. Each hexahedron element has nodes numbered 1, 2, 3, 4 and 5, 6, 7, 8 in a counter-clockwise manner, as shown in Figure 9.10.

As there are three DOFs at one node, there is a total of 24 DOFs in a hexahedron element. It is again useful to define a *natural coordinate system* (ξ, η, ζ) with its origin at the centre of the transformed cube, as this makes it easier to construct the shape functions and to evaluate the matrix integration. The coordinate mapping is performed in a similar manner as for quadrilateral elements in Chapter 7. Like the quadrilateral element, shape functions are also used to interpolate the coordinates from the nodal

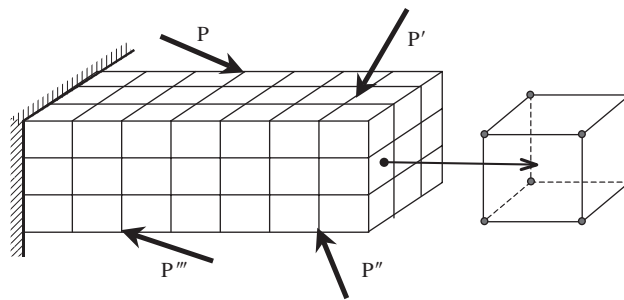


Figure 9.9. Solid block divided into eight-nodal hexahedron elements.

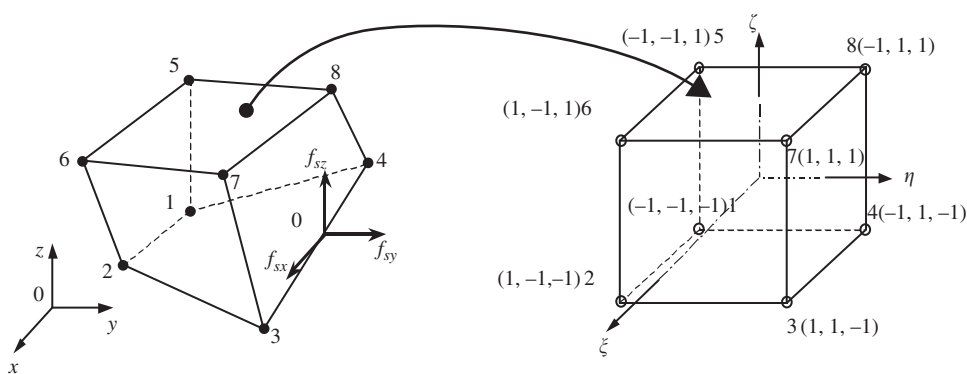


Figure 9.10. An eight-nodal hexahedron element and the coordinate systems.

coordinates:

$$\begin{aligned}
 x &= \sum_{i=1}^8 N_i(\xi, \eta, \zeta) x_i \\
 y &= \sum_{i=1}^8 N_i(\xi, \eta, \zeta) y_i \\
 z &= \sum_{i=1}^8 N_i(\xi, \eta, \zeta) z_i
 \end{aligned} \tag{9.34}$$

The shape functions are given in the local natural coordinate system as

$$\begin{aligned}
 N_1 &= \frac{1}{8}(1 - \xi)(1 - \eta)(1 - \zeta) \\
 N_2 &= \frac{1}{8}(1 + \xi)(1 - \eta)(1 - \zeta) \\
 N_3 &= \frac{1}{8}(1 + \xi)(1 + \eta)(1 - \zeta) \\
 N_4 &= \frac{1}{8}(1 - \xi)(1 + \eta)(1 - \zeta) \\
 N_5 &= \frac{1}{8}(1 - \xi)(1 - \eta)(1 + \zeta) \\
 N_6 &= \frac{1}{8}(1 + \xi)(1 - \eta)(1 + \zeta) \\
 N_7 &= \frac{1}{8}(1 + \xi)(1 + \eta)(1 + \zeta) \\
 N_8 &= \frac{1}{8}(1 - \xi)(1 + \eta)(1 + \zeta)
 \end{aligned} \tag{9.35}$$

or in a concise form,

$$N_i = \frac{1}{8}(1 + \xi_i \xi)(1 + \eta_i \eta)(1 + \zeta_i \zeta) \tag{9.36}$$

where (ξ_i, η_i, ζ_i) denotes the natural coordinates of node I .

From Eq. (9.36), it can be seen that the shape functions vary linearly in the ξ , η and ζ directions. Therefore, these shape functions are sometimes called tri-linear functions. The shape function N_i is a three-dimensional analogy of that given in Eq. (7.54). It is very easy to directly observe that the tri-linear elements possess the delta function property. In addition, since all these shape functions can be formed using the common set of eight basis functions of

$$1, \xi, \eta, \zeta, \xi\eta, \xi\zeta, \eta\zeta, \xi\eta\zeta \tag{9.37}$$

which contain both constant and linear basis functions. Therefore, these shape functions can expect to possess both partitions of the unity property as well as the linear reproduction property (see Lemmas 2 and 3 in Chapter 3).

In a hexahedron element, the displacement vector \mathbf{U} is a function of the coordinates x , y and z , and as before, it is interpolated using the shape functions

$$\mathbf{U} = \mathbf{N}\mathbf{d}_e \quad (9.38)$$

where the nodal displacement vector, \mathbf{d}_e is given by

$$\mathbf{d}_e = \begin{cases} \mathbf{d}_{e1} \\ \mathbf{d}_{e2} \\ \mathbf{d}_{e3} \\ \mathbf{d}_{e4} \\ \mathbf{d}_{e5} \\ \mathbf{d}_{e6} \\ \mathbf{d}_{e7} \\ \mathbf{d}_{e8} \end{cases} \begin{cases} \text{displacement components at node 1} \\ \text{displacement components at node 2} \\ \text{displacement components at node 3} \\ \text{displacement components at node 4} \\ \text{displacement components at node 5} \\ \text{displacement components at node 6} \\ \text{displacement components at node 7} \\ \text{displacement components at node 8} \end{cases} \quad (9.39)$$

in which

$$\mathbf{d}_{ei} = \begin{Bmatrix} u_1 \\ v_1 \\ w_1 \end{Bmatrix} \quad (i = 1, 2, \dots, 8) \quad (9.40)$$

is the displacement at node i . The matrix of shape functions is given by

$$\mathbf{N} = [\mathbf{N}_1 \quad \mathbf{N}_2 \quad \mathbf{N}_3 \quad \mathbf{N}_4 \quad \mathbf{N}_5 \quad \mathbf{N}_6 \quad \mathbf{N}_7 \quad \mathbf{N}_8] \quad (9.41)$$

in which each sub-matrix, \mathbf{N}_i , is given as

$$\mathbf{N}_i = \begin{bmatrix} N_i & 0 & 0 \\ 0 & N_i & 0 \\ 0 & 0 & N_i \end{bmatrix} \quad (i = 1, 2, \dots, 8) \quad (9.42)$$

In this case, the strain matrix defined by Eq. (9.17) can be expressed as

$$\mathbf{B} = [\mathbf{B}_1 \quad \mathbf{B}_2 \quad \mathbf{B}_3 \quad \mathbf{B}_4 \quad \mathbf{B}_5 \quad \mathbf{B}_6 \quad \mathbf{B}_7 \quad \mathbf{B}_8] \quad (9.43)$$

whereby

$$\mathbf{B}_i = \mathbf{L}\mathbf{N}_i = \begin{bmatrix} \partial N_i / \partial x & 0 & 0 \\ 0 & \partial N_i / \partial y & 0 \\ 0 & 0 & \partial N_i / \partial z \\ 0 & \partial N_i / \partial z & \partial N_i / \partial y \\ \partial N_i / \partial z & 0 & \partial N_i / \partial x \\ \partial N_i / \partial y & \partial N_i / \partial x & 0 \end{bmatrix} \quad (9.44)$$

As the shape functions are defined in terms of the natural coordinates, ξ , η and ζ , to obtain the derivatives with respect to x , y and z in the strain matrix, the chain rule of partial

differentiation needs to be used:

$$\begin{aligned}\frac{\partial N_i}{\partial \xi} &= \frac{\partial N_i}{\partial x} \frac{\partial x}{\partial \xi} + \frac{\partial N_i}{\partial y} \frac{\partial y}{\partial \xi} + \frac{\partial N_i}{\partial z} \frac{\partial z}{\partial \xi} \\ \frac{\partial N_i}{\partial \eta} &= \frac{\partial N_i}{\partial x} \frac{\partial x}{\partial \eta} + \frac{\partial N_i}{\partial y} \frac{\partial y}{\partial \eta} + \frac{\partial N_i}{\partial z} \frac{\partial z}{\partial \eta} \\ \frac{\partial N_i}{\partial \zeta} &= \frac{\partial N_i}{\partial x} \frac{\partial x}{\partial \zeta} + \frac{\partial N_i}{\partial y} \frac{\partial y}{\partial \zeta} + \frac{\partial N_i}{\partial z} \frac{\partial z}{\partial \zeta}\end{aligned}\quad (9.45)$$

which can be expressed in the matrix form

$$\begin{Bmatrix} \partial N_i / \partial \xi \\ \partial N_i / \partial \eta \\ \partial N_i / \partial \zeta \end{Bmatrix} = \mathbf{J} \begin{Bmatrix} \partial N_i / \partial x \\ \partial N_i / \partial y \\ \partial N_i / \partial z \end{Bmatrix}\quad (9.46)$$

where \mathbf{J} is the *Jacobian matrix* defined by

$$\mathbf{J} = \begin{bmatrix} \partial x / \partial \xi & \partial y / \partial \xi & \partial z / \partial \xi \\ \partial x / \partial \eta & \partial y / \partial \eta & \partial z / \partial \eta \\ \partial x / \partial \zeta & \partial y / \partial \zeta & \partial z / \partial \zeta \end{bmatrix}\quad (9.47)$$

Recall that the coordinates, x , y and z are interpolated by the shape functions from the nodal coordinates. Hence, substitute the interpolation of the coordinates, Eq. (9.34), into Eq. (9.47), which gives

$$\mathbf{J} = \begin{bmatrix} \frac{\partial N_1}{\partial \xi} & \frac{\partial N_2}{\partial \xi} & \frac{\partial N_3}{\partial \xi} & \frac{\partial N_4}{\partial \xi} & \frac{\partial N_5}{\partial \xi} & \frac{\partial N_6}{\partial \xi} & \frac{\partial N_7}{\partial \xi} & \frac{\partial N_8}{\partial \xi} \\ \frac{\partial N_1}{\partial \eta} & \frac{\partial N_2}{\partial \eta} & \frac{\partial N_3}{\partial \eta} & \frac{\partial N_4}{\partial \eta} & \frac{\partial N_5}{\partial \eta} & \frac{\partial N_6}{\partial \eta} & \frac{\partial N_7}{\partial \eta} & \frac{\partial N_8}{\partial \eta} \\ \frac{\partial N_1}{\partial \zeta} & \frac{\partial N_2}{\partial \zeta} & \frac{\partial N_3}{\partial \zeta} & \frac{\partial N_4}{\partial \zeta} & \frac{\partial N_5}{\partial \zeta} & \frac{\partial N_6}{\partial \zeta} & \frac{\partial N_7}{\partial \zeta} & \frac{\partial N_8}{\partial \zeta} \end{bmatrix} \begin{bmatrix} x_1 & y_1 & z_1 \\ x_2 & y_2 & z_2 \\ x_3 & y_3 & z_3 \\ x_4 & y_4 & z_4 \\ x_5 & y_5 & z_5 \\ x_6 & y_6 & z_6 \\ x_7 & y_7 & z_7 \\ x_8 & y_8 & z_8 \end{bmatrix}\quad (9.48)$$

or

$$\mathbf{J} = \begin{bmatrix} \sum_{i=1}^8 x_i \partial N_i / \partial \xi & \sum_{i=1}^8 y_i \partial N_i / \partial \xi & \sum_{i=1}^8 z_i \partial N_i / \partial \xi \\ \sum_{i=1}^8 x_i \partial N_i / \partial \eta & \sum_{i=1}^8 y_i \partial N_i / \partial \eta & \sum_{i=1}^8 z_i \partial N_i / \partial \eta \\ \sum_{i=1}^8 x_i \partial N_i / \partial \zeta & \sum_{i=1}^8 y_i \partial N_i / \partial \zeta & \sum_{i=1}^8 z_i \partial N_i / \partial \zeta \end{bmatrix}\quad (9.49)$$

Equation (9.46) can be re-written as

$$\begin{Bmatrix} \partial N_i / \partial x \\ \partial N_i / \partial y \\ \partial N_i / \partial z \end{Bmatrix} = \mathbf{J}^{-1} \begin{Bmatrix} \partial N_i / \partial \xi \\ \partial N_i / \partial \eta \\ \partial N_i / \partial \zeta \end{Bmatrix}\quad (9.50)$$

which is then used to compute the strain matrix, \mathbf{B} , in Eqs. (9.43) and (9.44), by replacing all the derivatives of the shape functions with respect to x , y and z to those with respect to ξ , η and ζ .

9.3.2 Element Matrices

Once the strain matrix, \mathbf{B} , has been computed, the stiffness matrix, \mathbf{k}_e , for 3D solid elements can be obtained by substituting \mathbf{B} into Eq. (3.71):

$$\mathbf{k}_e = \int_{V_e} \mathbf{B}^T \mathbf{c} \mathbf{B} dA = \int_{-1}^{+1} \int_{-1}^{+1} \int_{-1}^{+1} \mathbf{B}^T \mathbf{c} \mathbf{B} \det[\mathbf{J}] d\xi d\eta d\zeta \quad (9.51)$$

Note that the matrix of material constant, \mathbf{c} , is given by Eq. (2.9). As the strain matrix, \mathbf{B} , is a function of ξ , η and ζ , evaluating the integrations in Eq. (9.51) can be very difficult. Therefore, the integrals are performed using a numerical integration scheme. The Gauss integration scheme discussed in Section 7.3.4 is often used to carry out the integral. For three-dimensional integrations, the Gauss integration is sampled in three directions, as follows:

$$I = \int_{-1}^{+1} \int_{-1}^{+1} \int_{-1}^{+1} f(\xi, \eta) d\xi d\eta = \sum_{i=1}^n \sum_{j=1}^m \sum_{k=1}^l w_i w_j w_k f(\xi_i, \eta_j, \zeta_k) \quad (9.52)$$

To obtain the mass (inertia) matrix for the hexahedron element, substitute the shape function matrix, Eq. (9.41), into Eq. (3.75):

$$\mathbf{m}_e = \int_{V_e} \rho \mathbf{N}^T \mathbf{N} dV = \int_{-1}^1 \int_{-1}^1 \int_{-1}^1 \rho \mathbf{N}^T \mathbf{N} \det[\mathbf{J}] d\xi d\eta d\zeta \quad (9.53)$$

The above integral is also usually carried out using Gauss integration. If the hexahedron is rectangular with dimensions of $a \times b \times c$, the determinate of the Jacobian matrix is simply given by

$$\det[\mathbf{J}] = abc = V_e \quad (9.54)$$

and the mass matrix can be explicitly obtained as

$$\mathbf{m}_e = \begin{bmatrix} \mathbf{m}_{11} & \mathbf{m}_{12} & \mathbf{m}_{13} & \mathbf{m}_{14} & \mathbf{m}_{15} & \mathbf{m}_{16} & \mathbf{m}_{17} & \mathbf{m}_{18} \\ & \mathbf{m}_{22} & \mathbf{m}_{23} & \mathbf{m}_{24} & \mathbf{m}_{25} & \mathbf{m}_{26} & \mathbf{m}_{27} & \mathbf{m}_{28} \\ & & \mathbf{m}_{33} & \mathbf{m}_{34} & \mathbf{m}_{35} & \mathbf{m}_{36} & \mathbf{m}_{37} & \mathbf{m}_{38} \\ & & & \mathbf{m}_{44} & \mathbf{m}_{45} & \mathbf{m}_{46} & \mathbf{m}_{47} & \mathbf{m}_{48} \\ & & & & \mathbf{m}_{55} & \mathbf{m}_{56} & \mathbf{m}_{57} & \mathbf{m}_{58} \\ & & & & & \mathbf{m}_{66} & \mathbf{m}_{67} & \mathbf{m}_{68} \\ & & & & & & \mathbf{m}_{77} & \mathbf{m}_{78} \\ & & & & & & & \mathbf{m}_{88} \end{bmatrix} \quad (9.55)$$

.sy.

where

$$\begin{aligned}
 \mathbf{m}_{ij} &= \int_{-1}^1 \int_{-1}^1 \int_{-1}^1 \rho abc \mathbf{N}_i \mathbf{N}_j d\xi d\eta d\zeta \\
 &= \rho abc \int_{-1}^1 \int_{-1}^1 \int_{-1}^1 \begin{bmatrix} N_i & 0 & 0 \\ 0 & N_i & 0 \\ 0 & 0 & N_i \end{bmatrix} \begin{bmatrix} N_j & 0 & 0 \\ 0 & N_j & 0 \\ 0 & 0 & N_j \end{bmatrix} d\xi d\eta d\zeta \\
 &= \rho abc \int_{-1}^1 \int_{-1}^1 \int_{-1}^1 \begin{bmatrix} N_i N_j & 0 & 0 \\ 0 & N_i N_j & 0 \\ 0 & 0 & N_i N_j \end{bmatrix} d\xi d\eta d\zeta \quad (9.56)
 \end{aligned}$$

or

$$\mathbf{m}_{ij} = \begin{bmatrix} m_{ij} & 0 & 0 \\ 0 & m_{ij} & 0 \\ 0 & 0 & m_{ij} \end{bmatrix} \quad (9.57)$$

in which

$$\begin{aligned}
 m_{ij} &= \rho abc \int_{-1}^{+1} \int_{-1}^{+1} N_i N_j d\xi d\eta d\zeta \\
 &= \frac{\rho abc}{64} \int_{-1}^{+1} (1 + \xi_i \xi)(1 + \xi_j \xi) d\xi \int_{-1}^{+1} (1 + \eta_i \eta)(1 + \eta_j \eta) d\eta \\
 &\quad \times \int_{-1}^{+1} (1 + \zeta_i \zeta)(1 + \zeta_j \zeta) d\zeta \\
 &= \frac{\rho hab}{8} \left(1 + \frac{1}{3} \xi_i \xi_j\right) \left(1 + \frac{1}{3} \eta_i \eta_j\right) \left(1 + \frac{1}{3} \zeta_i \zeta_j\right) \quad (9.58)
 \end{aligned}$$

As an example, m_{33} is calculated as follows:

$$m_{33} = \frac{\rho abc}{8} \left(1 + \frac{1}{3} \times 1 \times 1\right) \left(1 + \frac{1}{3} \times 1 \times 1\right) \left(1 + \frac{1}{3} \times 1 \times 1\right) = 8 \times \frac{\rho abc}{216} \quad (9.59)$$

The other components of the mass matrix for a rectangular hexahedron element are:

$$\begin{aligned}
 m_{11} &= m_{22} = m_{33} = m_{44} = m_{55} = m_{66} = m_{77} = m_{88} = \frac{8\rho abc}{216} \\
 m_{12} &= m_{23} = m_{34} = m_{56} = m_{67} = m_{78} = m_{14} = m_{58} = m_{15} = m_{26} = m_{37} \\
 &= m_{48} = \frac{4\rho abc}{216} \\
 m_{13} &= m_{24} = m_{16} = m_{25} = m_{36} = m_{47} = m_{57} = m_{68} = m_{27} = m_{38} = m_{45} \\
 &= m_{18} = \frac{2\rho abc}{216} \\
 m_{17} &= m_{28} = m_{35} = m_{46} = \frac{1\rho abc}{216}
 \end{aligned} \quad (9.60)$$

Note that the equalities in the above equation can be easily figured out by observing the relative geometric positions of the nodes in the cube element. For example, the relative geometric positions of nodes 1–2 is equivalent to the relative geometric positions of nodes 2–3, and the relative geometric positions of nodes 1–7 is equivalent to the relative geometric positions of nodes 2–8. If we write the portion of the mass matrix corresponding to only one translational direction, say the x direction, we have

$$\mathbf{m}_e = \frac{\rho abc}{216} \begin{bmatrix} 8 & 4 & 2 & 4 & 4 & 2 & 1 & 2 \\ & 8 & 4 & 2 & 2 & 4 & 2 & 1 \\ & & 8 & 4 & 1 & 2 & 4 & 2 \\ & & & 8 & 2 & 1 & 2 & 4 \\ & & & & 8 & 4 & 2 & 4 \\ & & & & & 8 & 4 & 2 \\ & & & & & & 8 & 4 \\ & & & & & & & 8 \end{bmatrix} \quad (9.61)$$

The mass matrices corresponding to only the y and z directions are exactly the same as \mathbf{m}_e .

The nodal force vector for a rectangular hexahedron element can be obtained using Eqs. (3.78), (3.79) and (3.81). Suppose the element is loaded by a distributed force \mathbf{f}_s on edge 3–4 of the element, as shown in Figure 9.10; the nodal force vector becomes

$$\mathbf{f}_e = \int_l [\mathbf{N}]^T|_{3-4} \begin{Bmatrix} f_{sx} \\ f_{sy} \\ f_{sz} \end{Bmatrix} dl \quad (9.62)$$

If the load is uniformly distributed, f_{sx} , f_{sy} and f_{sz} are constants, and the above equation becomes

$$\mathbf{f}_e = \frac{1}{2} l_{3-4} \begin{Bmatrix} \{\mathbf{0}\}_{3 \times 1} \\ \{\mathbf{0}\}_{3 \times 1} \\ \begin{Bmatrix} f_{sx} \\ f_{sy} \\ f_{sz} \end{Bmatrix} \\ \begin{Bmatrix} f_{sx} \\ f_{sy} \\ f_{sz} \end{Bmatrix} \\ \{\mathbf{0}\}_{3 \times 1} \\ \{\mathbf{0}\}_{3 \times 1} \\ \{\mathbf{0}\}_{3 \times 1} \\ \{\mathbf{0}\}_{3 \times 1} \end{Bmatrix} \quad (9.63)$$

where l_{3-4} is the length of edge 3–4. Equation (9.63) implies that the distributed forces are equally divided and applied at the two nodes. This conclusion suggests also to evenly distribute surface forces applied on any face of the element, and to evenly distribute body forces applied on the entire body of the element.

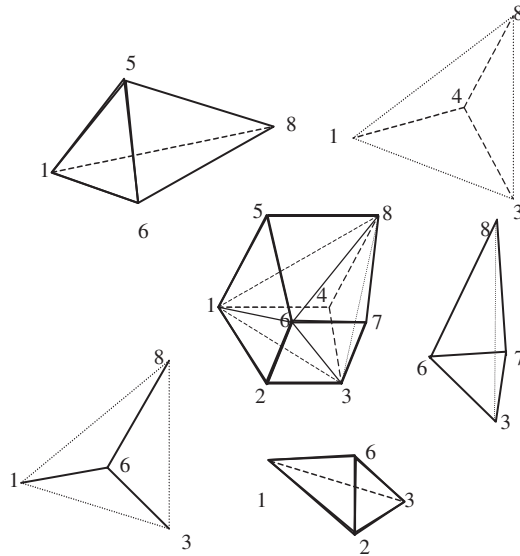


Figure 9.11. A hexahedron broken up into five tetrahedrons.

9.3.3 Using Tetrahedrons to form Hexahedrons

An alternative method of formulating hexahedron elements is to make use of tetrahedron elements. This is built upon the fact that a hexahedron can be said to be made up of numerous tetrahedrons. Figure 9.11 shows how a hexahedron can be made up of five tetrahedrons. Of course, this is not the only way that a hexahedron can be made up of five tetrahedrons, and it can also be made up of six tetrahedrons, as shown in Figure 9.12. Similarly, there is more than one way of dividing a hexahedron into six tetrahedrons. In this way, the element matrices for a hexahedron can be formed by assembling all the matrices for the tetrahedron elements, each of which is developed in Section 9.2.2. The assembly is done in a similar way to the assembly between elements.

9.4 HIGHER ORDER ELEMENTS

9.4.1 Tetrahedron Elements

Two higher order tetrahedron elements with 10 and 20 nodes are shown in Figures 9.13(a) and (b), respectively. The 10-node tetrahedron element is a quadratic element. Compared with the linear tetrahedron element (four-nodal) developed earlier, six additional nodes are added at the middle of the edges of the element. In developing the 10-nodal tetrahedron element, a complete polynomial up to second order can be used. The shape functions for

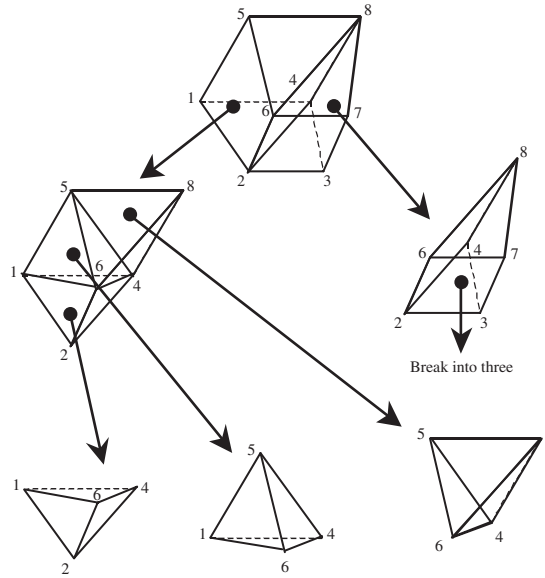


Figure 9.12. A hexahedron broken up into six tetrahedrons.

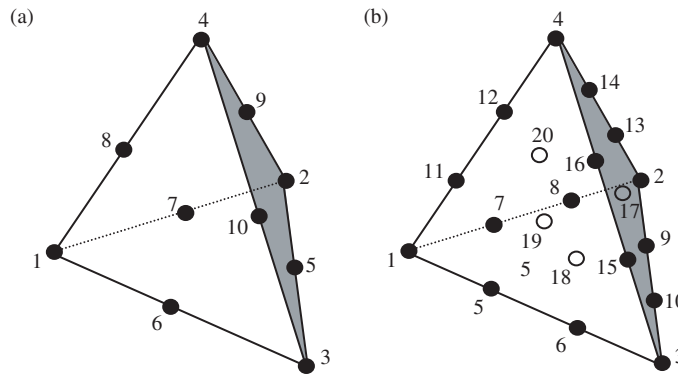


Figure 9.13. Higher order 3D tetrahedron elements. (a) 10-node tetrahedron element; (b) 20-node tetrahedron element.

this quadratic tetrahedron element in the volume coordinates are given as follows:

$$\left. \begin{aligned}
 N_i &= (2L_i - 1)L_i && \text{for corner nodes } i = 1, 2, 3, 4 \\
 N_5 &= 4L_2L_3 \\
 N_6 &= 4L_1L_3 \\
 N_7 &= 4L_1L_2 \\
 N_8 &= 4L_1L_4 \\
 N_9 &= 4L_2L_4 \\
 N_{10} &= 4L_3L_4
 \end{aligned} \right\} \text{for mid-edge nodes} \tag{9.64}$$

where L_i is the volume coordinate, which is the same as the shape function for the linear tetrahedron elements given by Eq. (9.15).

The 20-node tetrahedron element is a cubic element. Compared with the linear tetrahedron element (four-nodal) developed earlier, two additional nodes are added evenly on each edge of the element, and four-node central-face nodes are added at the geometry centre of each triangular surface of the element. In developing the 20-nodal tetrahedron element, a complete polynomial up to third order can be used. The shape functions for this cubic tetrahedron element in the volume coordinates are given as follows:

$$\begin{aligned}
 N_i &= \frac{1}{2}(3L_i - 1)(3L_i - 2)L_i \quad \text{for corner nodes } i = 1, 2, 3, 4 \\
 N_5 &= \frac{9}{2}(3L_1 - 1)L_1L_3 & N_{11} &= \frac{9}{2}(3L_1 - 1)L_1L_4 \\
 N_6 &= \frac{9}{2}(3L_3 - 1)L_1L_3 & N_{12} &= \frac{9}{2}(3L_4 - 1)L_1L_4 \\
 N_7 &= \frac{9}{2}(3L_1 - 1)L_1L_2 & N_{13} &= \frac{9}{2}(3L_2 - 1)L_2L_4 \\
 N_8 &= \frac{9}{2}(3L_2 - 1)L_1L_2 & N_{14} &= \frac{9}{2}(3L_4 - 1)L_2L_4 \\
 N_9 &= \frac{9}{2}(3L_2 - 1)L_2L_3 & N_{15} &= \frac{9}{2}(3L_3 - 1)L_3L_4 \\
 N_{10} &= \frac{9}{2}(3L_3 - 1)L_2L_3 & N_{16} &= \frac{9}{2}(3L_4 - 1)L_3L_4
 \end{aligned}
 \left. \vphantom{\begin{aligned} N_5 \\ N_6 \\ N_7 \\ N_8 \\ N_9 \\ N_{10} \end{aligned}} \right\} \text{for edge nodes} \tag{9.65}$$

$$\left. \begin{aligned}
 N_{17} &= 27L_2L_3L_4 \\
 N_{18} &= 27L_1L_2L_3 \\
 N_{19} &= 27L_1L_3L_4 \\
 N_{20} &= 27L_1L_2L_4
 \end{aligned} \right\} \text{for centre surface nodes}$$

where L_i is the volume coordinate, which is the same as the shape function for the linear tetrahedron elements given by Eq. (9.15).

9.4.2 Brick Elements

Lagrange type elements

The Lagrange type brick elements can be developed in precisely the same manner as the 2D rectangular elements described in Chapter 7. Consider a brick element with $n_d = (n + 1)(m + 1)(p + 1)$ nodes shown in Figure 9.14. The element is defined in the domain of $(-1 \leq \xi \leq 1, -1 \leq \eta \leq 1, -1 \leq \zeta \leq 1)$ in the natural coordinates ξ , η and ζ . Due to the regularity of the nodal distribution along the ξ , η and ζ directions, the shape function of the element can be simply obtained by multiplying one-dimensional shape functions with respect to the ξ , η and ζ directions using the Lagrange interpolants defined in Eq. (4.82) [Zienkiewicz *et al.*, 2000]:

$$N_i = N_I^{1D} N_J^{1D} N_K^{1D} = l_I^n(\xi) l_J^m(\eta) l_K^p(\zeta) \tag{9.66}$$

Due to the delta function property of the 1D shape functions given in Eq. (4.83), it is easy to confirm that the N_i given by Eq. (9.66) also has the delta function property.

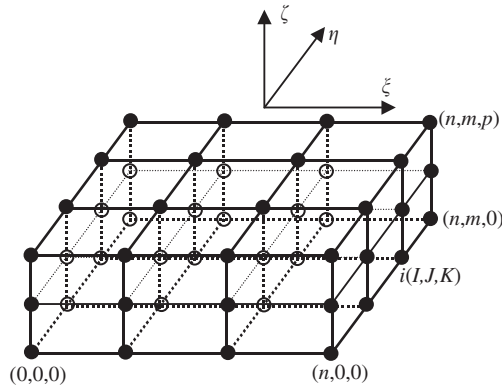


Figure 9.14. Brick element of arbitrary high orders.

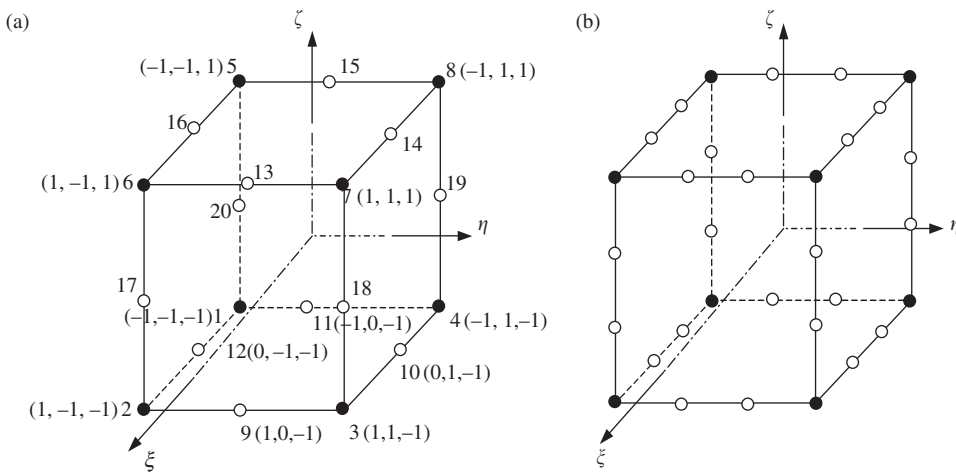


Figure 9.15. High order 3D serendipity elements. (a) 20-node quadratic element; (b) 32-node cubic element.

Serendipity type elements

The method used in constructing the Lagrange type of elements is very systematic. However, the Lagrange type of elements is not very widely used, due to the presence of the interior nodes. A serendipity type of brick elements without interior nodes is created by inspective construction methods as described in Chapter 7 for 2D rectangular elements.

Figure 9.15(a) shows a 20-nodal tri-quadratic element. The element has eight corner nodes and twelve mid-side nodes. The shape functions in the natural coordinates for the

quadratic brick element are given as follows:

$$\begin{aligned}
 N_j &= \frac{1}{8}(1 + \xi_j \xi)(1 + \eta_j \eta)(1 + \zeta_j \zeta)(\xi_j \xi + \eta_j \eta + \zeta_j \zeta - 2) && \text{for corner nodes } j = 1, \dots, 8 \\
 N_j &= \frac{1}{4}(1 - \xi^2)(1 + \eta_j \eta)(1 + \zeta_j \zeta) && \text{for mid-side nodes } j = 10, 12, 14, 16 \\
 N_j &= \frac{1}{4}(1 - \eta^2)(1 + \xi_j \xi)(1 + \zeta_j \zeta) && \text{for mid-side nodes } j = 9, 11, 13, 15 \\
 N_j &= \frac{1}{4}(1 - \zeta^2)(1 + \xi_j \xi)(1 + \eta_j \eta) && \text{for mid-side nodes } j = 17, 18, 19, 20
 \end{aligned} \tag{9.67}$$

where (ξ_j, η_j) are the natural coordinates of node j . It is very easy to observe that the shape functions possess the delta function property. The shape function is constructed by simple inspections, making use of the shape function properties. For example, for corner node 2 (where $\xi_2 = 1, \eta_2 = -1, \zeta_2 = -1$), the shape function N_2 has to pass the following four planes as shown in Figure 9.16 to ensure its vanishing at remote nodes:

$$\begin{aligned}
 1 + \xi = 0 &\Rightarrow \text{vanishes at nodes } 1, 4, 5, 8, 11, 15, 19, 20 \\
 \eta - 1 = 0 &\Rightarrow \text{vanishes at nodes } 3, 4, 7, 8, 10, 14, 18, 19 \\
 \zeta - 1 = 0 &\Rightarrow \text{vanishes at nodes } 5, 6, 7, 8, 13, 14, 15, 16 \\
 \xi - \eta - \zeta - 2 = 0 &\Rightarrow \text{vanishes at nodes } 9, 12, 17
 \end{aligned} \tag{9.68}$$

The shape N_2 can then be immediately written as

$$N_2 = C(1 + \xi)(1 - \eta)(1 - \zeta)(\xi - \eta - \zeta - 2) \tag{9.69}$$

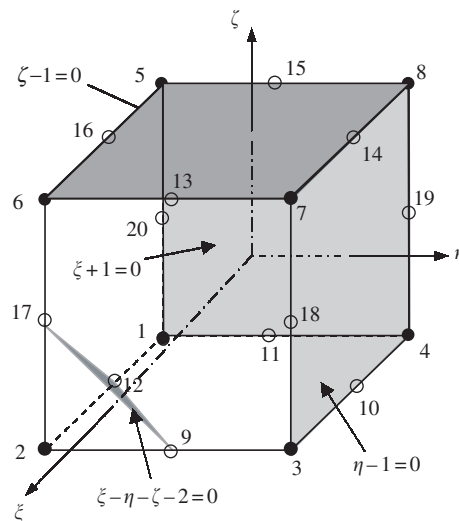


Figure 9.16. Construction of 20-node serendipity element. Four flat planes passing through the remote nodes of node 2 are used.

where C is a constant to be determined using the condition that it has to be unity at node 2 at $(\xi_2 = 1, \eta_2 = -1, \zeta_2 = -1)$, which gives

$$C = \frac{1}{(1 + 1)(1 - (-1))(1 - (-1))(1 - (-1) - (-1) - 2)} = \frac{1}{8} \quad (9.70)$$

We finally have

$$N_2 = \frac{1}{8}(1 + \xi_2\xi)(1 + \eta_2\eta)(1 + \zeta_2\zeta)(\xi_2\xi + \eta_2\eta + \zeta_2\zeta - 2) \quad (9.71)$$

which is the first equation in Eq. (9.67) for $j = 1$.

Shape functions at all the other corner nodes can be constructed in exactly the same manner. As for the mid-side nodes, say node 9, we enforce the shape function passing through the following four planes, as shown Figure 9.17.

$$\begin{aligned} 1 + \xi = 0 &\Rightarrow \text{vanishes at nodes 1, 4, 5, 8, 11, 15, 19, 20} \\ \eta - 1 = 0 &\Rightarrow \text{vanishes at nodes 3, 4, 7, 8, 10, 14, 18, 19} \\ \zeta - 1 = 0 &\Rightarrow \text{vanishes at nodes 5, 6, 7, 8, 13, 14, 15, 16} \\ \eta + 1 = 0 &\Rightarrow \text{vanishes at nodes 1, 2, 5, 6, 12, 13, 16, 17} \end{aligned} \quad (9.72)$$

The shape N_9 can then be immediately written as

$$N_9 = C(1 - \eta^2)(1 + \xi)(1 - \zeta) \quad (9.73)$$

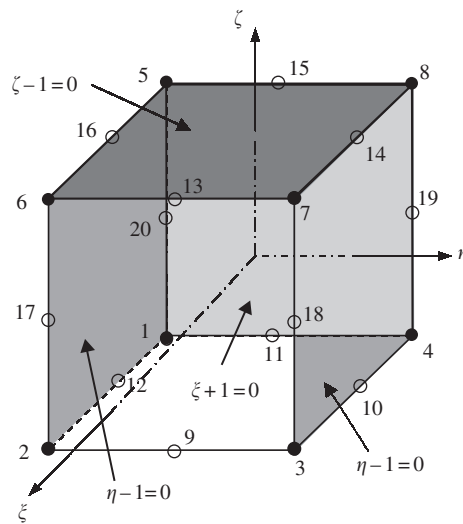


Figure 9.17. Construction of 20-node serendipity element. Four flat planes passing through the remote nodes of node 2 are used.

where C is a constant to be determined using the condition that it has to be unity at node 5 at $(\xi_9 = 1, \eta_9 = 0, \zeta_9 = -1)$, which gives

$$C = \frac{1}{(1 - \eta^2)(1 + \xi)(1 - \zeta)} = \frac{1}{(1 - 0^2)(1 + 1)(1 - (-1))} = \frac{1}{4} \quad (9.74)$$

We finally have

$$N_9 = \frac{1}{4}(1 - \eta^2)(1 + \xi_9\xi)(1 + \zeta_9\zeta) \quad (9.75)$$

which is the third equation in Eq. (9.67) for $j = 9$.

Because the delta function property is used for the construction of shape functions given in Eq. (9.67), they of course, possess, the delta function property. It can easily be seen that all the shape functions can be formed using the following common set of basis functions:

$$\begin{aligned} &1, \xi, \eta, \zeta\xi\eta, \eta\zeta, \xi\zeta, \xi^2, \eta^2, \zeta^2, \\ &\xi\eta\zeta, \xi\eta^2, \xi\zeta^2, \eta\xi^2, \eta\zeta^2, \zeta\xi^2, \zeta\eta^2, \xi^2\eta\zeta, \eta^2\xi\zeta, \xi\eta\zeta^2 \end{aligned} \quad (9.76)$$

that are linearly-independent and contain all the linear terms. From Lemmas 2 and 3, we confirm that the shape functions are partitions of unity, and at least linear field reproduction. Hence, they satisfy the sufficient requirements for FEM shape functions.

Following the similar procedure, the shape functions for the 32-node tri-cubic element shown in Figure 9.15(b) can be written as

$$\begin{aligned} N_j &= \frac{1}{64}(1 + \xi_j\xi)(1 + \eta_j\eta)(1 + \zeta_j\zeta)(9\xi^2 + 9\eta^2 + 9\zeta^2 - 19) \\ &\quad \text{for corner nodes } j = 1, \dots, 8 \\ N_j &= \frac{9}{64}(1 - \xi^2)(1 + 9\xi_j\xi)(1 + \eta_j\eta)(1 + \zeta_j\zeta) \\ &\quad \text{for side nodes with } \xi_j = \pm\frac{1}{3}, \eta_j = \pm 1 \text{ and } \zeta_j = \pm 1 \\ N_j &= \frac{9}{64}(1 - \eta^2)(1 + 9\eta_j\eta)(1 + \xi_j\xi)(1 + \zeta_j\zeta) \\ &\quad \text{for side nodes with } \eta_j = \pm\frac{1}{3}, \xi_j = \pm 1 \text{ and } \zeta_j = \pm 1 \\ N_j &= \frac{9}{64}(1 - \zeta^2)(1 + 9\zeta_j\zeta)(1 + \xi_j\xi)(1 + \eta_j\eta) \\ &\quad \text{for side nodes with } \zeta_j = \pm\frac{1}{3}, \xi_j = \pm 1 \text{ and } \eta_j = \pm 1 \end{aligned} \quad (9.77)$$

The reader is encouraged to figure out what are the planes that should be used to form the shape functions listed in Eq. (9.77). When $\zeta = \zeta_i = 1$, the above equations reduce to a two-dimensional case of serendipity quadratic and cubic elements defined by Eqs. (7.107), (7.111) and (7.113).

9.5 ELEMENTS WITH CURVED SURFACES

Using high order elements, elements with curved surfaces can be used in the modelling. Two relatively frequently used higher order elements of curved edges are shown in Figure 9.18(a). In formulating these types of elements, the same mapping technique used for the linear